WILEY

^{15}N hyperpolarisation of the antiprotozoal drug ornidazole by Signal Amplification By Reversible Exchange in aqueous medium

Wissam Iali[1] | Gamal A. I. Moustafa[2,3] | Laurynas Dagys[3] | Soumya S. Roy[3] 🆔

[1]Department of Chemistry, King Fahd University of Petroleum and Minerals (KFUPM), Dhahran, Saudi Arabia

[2]Department of Medicinal Chemistry, Faculty of Pharmacy, Minia University, Minia, Egypt

[3]School of Chemistry, University of Southampton, Southampton, UK

Correspondence
Soumya S. Roy, School of Chemistry, University of Southampton, University Road, Southampton, SO17 1BJ, UK.
Email: s.s.roy@soton.ac.uk

Abstract

Signal amplification by reversible exchange (SABRE) offers a cost-effective route to boost nuclear magnetic resonance (NMR) signal by several orders of magnitude by employing readily available *para*-hydrogen as a source of hyperpolarisation. Although ^{1}H spins have been the natural choice of SABRE hyperpolarisation since its inception due to its simplicity and accessibility, limited spin lifetimes of ^{1}H makes it harder to employ them in a range of time-dependent NMR experiments. Heteronuclear spins, for example, ^{13}C and ^{15}N, in general have much longer T_1 lifetimes and thereby are found to be more suitable for hyperpolarised biological applications as demonstrated previously by *para*-hydrogen induced polarisation (PHIP) and dynamic nuclear polarisation (DNP). In this study we demonstrate a simple procedure to enhance ^{15}N signal of an antibiotic drug ornidazole by up to 71,000-folds with net ^{15}N polarisation reaching ∼23%. Further, the effect of co-ligand strategy is studied in conjunction with the optimum field transfer protocols and consequently achieving ^{15}N hyperpolarised spin lifetime of >3 min at low field. Finally, we present a convenient route to harness the hyperpolarised solution in aqueous medium free from catalyst contamination leading to a strong ^{15}N signal detection for an extended duration of time.

1 | INTRODUCTION

Nuclear magnetic resonance (NMR) is one of the most versatile analytical techniques in physical science, but it suffers from low sensitivity that is due to a weak net magnetisation dictated by the thermal equilibrium. At room temperature and within a 9.4 T magnet, only 1 out of ∼32,000 ^{1}H spins effectively contribute towards the NMR signal detection. The spin distribution is even more abject in the cases of low-gamma spins, for example, ^{13}C and ^{15}N, where in the latter case, only 1 out of ∼300,000

^{15}N nuclei effectively participates in signal emission in a 9.4 T magnet.

In recent years, hyperpolarisation (HP) techniques have made significant advances circumventing the issue of poor thermal polarisation of nuclear spins and successfully demonstrated that NMR signals of a large class of important molecular targets can be enhanced by several orders of magnitude.[1,2] Among the techniques available, dynamic nuclear polarisation (DNP) has made significant inroad towards the magnetic resonance imaging (MRI) applications by producing ^{13}C-enhanced metabolites of high

significance.[3] However, DNP is often technologically demanding method that also involves slow polarisation process which makes it less accessible.[4] An alternative HP method of *para*-hydrogen (pH$_2$) induced polarisation (PHIP) is particularly useful due to its minimal instrumentation and fast delivery.[5,6] The method uses easy-to-attain *para*-enriched hydrogen (*para*-hydrogen) gas and some chemical interaction to utilise its nuclear singlet order for the target spins.[7] Although classically PHIP employs hydrogenation reaction, an attractive non-hydrogenative method of signal amplification by reversible exchange (SABRE) was developed which allows to repeat the process without causing any chemical modification of the molecular precursor.[8–14] The target spins of SABRE are not only limited to ^{1}H as further techniques such as SABRE-SHEATH (SABRE in SHield Enables Alignment Transfer to Heteronuclei) have been introduced to hyperpolarise heteronuclei.[14–26]

Nitrogen containing targets are particularly interesting because of their presence in biomolecules in conjunction with their longer relaxation times as compared to ^{1}H and ^{13}C. SABRE-SHEATH have granted with ^{15}N polarisation in the excess of 20% in a variety of biomolecules.[12,16,17,21,27] In addition, when SABRE was coupled with long-lived singlet states (LLS), a significant extension in HP spin lifetimes were seen with reported ^{15}N decay constant of ∼20 min in the cases of ^{15}N$_2$-diazirin tags.[28] In comparison, hyperpolarising ^{15}N targets by DNP was found to be much less efficient and challenging compared to more successful ^{13}C targets with a maximum ^{15}N polarisation levels reported ca. 3% in the case of ^{15}N-choline.[29,30] However, an impressive ∼15 min ^{15}N HP lifetime was reported by Nonaka et al. in conjunction with the DNP technique based on suitable synthetic targets.[31]

In this study we report ∼23% ^{15}N polarisation in the sample of 50 mM ornidazole (Odz) only using 50% *para*-enriched hydrogen gas. Ornidazole is a nitroimidazole based drug and was selected for the study for its common use as antibiotic for treating a range of anaerobic bacterial infections.[32–34] Our study also reveals that it is possible to not only to highly polarise this drug but also to separate it from the heavy metal catalyst using the technique of phase extraction. The results further indicate that this and other related drugs could be potentially prepared for biomedical use in a cheap and cost-effective way by using PHIP and SABRE.

2 | RESULTS AND DISCUSSIONS

2.1 | Equipment and preparation

All the HP experiments in this work were performed using a custom built *para*-hydrogen (pH$_2$) generator producing ∼50% enriched pH$_2$ when H$_2$ is passed through iron (III) oxide catalyst cooled by liquid nitrogen bath. Samples for the study were prepared by mixing 5 mM of [IrCl (COD)(IMes)] (IMes = 1,3-bis[2,4,6-trimethylphenyl]imidazol-2-ylidene) catalyst with 50 mM of Odz) in 0.6 ml of solvents specified in the following subsections.[35] After degassing, samples were activated by filling the J-Young's tube with pH$_2$ with 4 bar of pressure and subsequently mixing the solutions by shaking vigorously at magnetic field of choice. Low magnetic field for SABRE-SHEATH method was generated by a solenoid coil put in a multi-layer mu-metal chamber. Fields in the region of mT were achieved using the stray field of the magnet. All NMR data was collected with a 400 MHz Bruker spectrometer (unless otherwise stated) at an ambient temperature of 298 K.

2.2 | Hyperpolarising ^{1}H and ^{15}N by SABRE and SABRE-SHEATH

Ornidazole contains three nitrogen sites (Scheme 1) and similar targets of imidazole motifs including metronidazole and nimorazole have been shown to hyperpolarise well via SABRE.[16,18,19,21,27,36,37] The imidazole motif is present in a range of pharmacologically active agents,
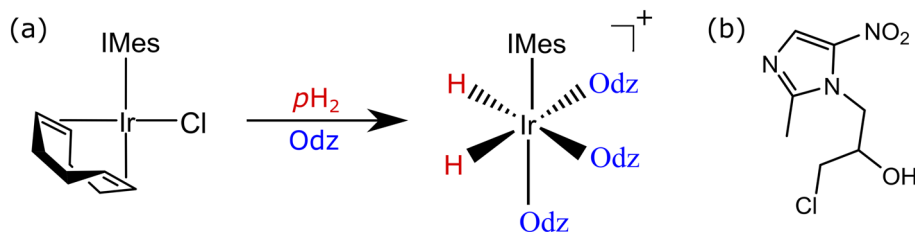
SCHEME 1 (a) Schematic of the SABRE method of ornidazole (Odz). Both pH$_2$ and substrate (Odz) bind to the Ir-IMes catalyst for a reversible chemical exchange to transfer nuclear spin order from the hydrides to the target nuclei of Odz via *J*-coupling network when resonance matching conditions are met. (b) Chemical structure of ornidazole (Odz) whose α-nitrogen site binds to the Iridium metal centre in a reversible fashion

and therefore, screening their NMR detection and magnetic state lifetimes is an active field of research in itself.[37,38] Scheme 1 depicts the SABRE mechanism where Odz binds to the catalyst through the less sterically hindered nitrogen (α-nitrogen) reversibly to forge a polarisation transfer pathway (based on *J*-coupling network) with the hydrides when both are bound. The relatively strong coupling constant between the hydrides and the nitrogen ($^2J_{1H-15N} \approx 25$ Hz) thus is critical towards driving the polarisation to the target spins of Odz. However, in the cases of heteronuclei targets, a microtesla (μT) field is required (∼100 times below the Earth's magnetic field) to fulfil the condition of polarisation transfer and the process is termed as SABRE-SHEATH.[15,39] When Odz binds to the iridium, it forms a AAX type spin system and the polarisation transfer occurs when all three spins are strongly coupled, meaning that the difference in their NMR frequencies is smaller than or comparable to both significant couplings within the spin system, i.e., J_{HH} and J_{NH}. This condition can be met either by performing the SABRE reaction at microtesla fields or at high fields with suitable radio frequency pulses. We followed the low-field spontaneous approach in this study.[15,39–41]

2.2.1 | ¹H SABRE

First, SABRE effect to polarise ¹H of the Odz was examined. *Sample-1* was prepared with 5 mM of iridium catalyst and 50 mM of Odz dissolved in 0.6 ml of methanol-d_4 (CD$_3$OD). After degassing the solution by three cycles of freeze–pump–thaw method, the tube was filled with pH_2 of 50% enrichment under 4 bar of pressure. Figure 1a displays the ¹H SABRE HP effect

when the sample tube was shaken at a stray field of ∼6 mT for ∼10 s before dropping it inside the magnet for signal detection. A modest 8-folds enhancement factor was achieved for the imidazole proton, originating from direct polarisation transfer via 4-bonds *J*-coupling (∼1.0 Hz) from the hydrides. A much weaker 5-bonds *J*-coupling (<0.5 Hz) was proved insufficient to observe any signal enhancement for the methyl protons. The enhancement factor for ¹H was calculated by taking the integrals of the hyperpolarised peaks compared to thermal signal. Figure 1b illustrates the formation of a typical SABRE active species [Ir(H)$_2$(IMes)(Odz)$_3$]Cl as the main product as confirmed by characterising two equivalent hydride ligands peaks at −25.90 ppm (see Supporting Information [SI] for more details on peak assignments). The weak ¹H enhancement of free Odz can be attributed to the fast exchange process of the substrate with the metal centre in conjunction with the fast relaxation of ¹H nuclei under this condition.

2.2.2 | Co-ligand strategy

Recently, the development of co-ligand strategy have expanded the scopes of SABRE where suitable ligand design route facilitated hyperpolarising highly important molecules, for example, pyruvate, acetate and glucose.[14,20,42] Earlier, Shchepin et al., has described a similar approach called 'pyridine aided activation' that improves the efficacy of SABRE process to nicotinamide.[43] This stems from the fact that a suitable co-ligand can provide the desired stabilisation to the active species when a substrate binds to the iridium metal centre very weakly. Among the various co-ligands employed,
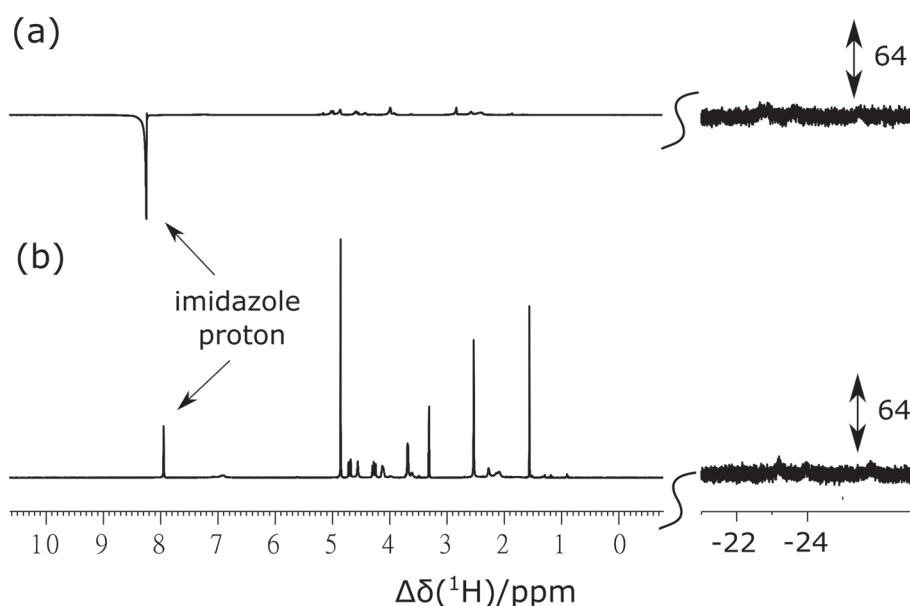
FIGURE 1 (a) ¹H NMR spectra associated with 50 mM Odz mixed with 5 mM catalyst in 0.6 ml CD$_3$OD solution and resulting in (a) SABRE hyperpolarised spectrum when mixed with pH_2 at ∼6 mT stray magnetic field for ∼10 s and (b) corresponding signals at thermal equilibrium (one scan). The hydride regions are scaled vertically by 64 times compared to the rest of the spectra

amines and dimethyl sulfoxide (DMSO) were found to be widely suitable for many of the substrates that were earlier found to be challenging with SABRE mechanism.[44,45] Recently, Fekete et al described the efficacy of such strategy where benzylamine-d_7 was employed to boost the ^{15}N signal enhancement of metronidazole by at least double when compared to usual SABRE-SHEATH without any co-ligands.[27]

In this work, we prepared *sample-2* by adding benzylamine (BnNH$_2$) as a co-ligand with a ratio of 1:10:3.5 respectively to the catalyst: Odz:BnNH$_2$ and dissolving it in CD$_3$OD.[11,44] Upon performing SABRE with this sample, we however, observed only a slight increase in the ^1H signal enhancement up to 23-folds to the imidazole proton and 2-folds for the methyl protons. In addition, a fast H/D exchange was noticed examining the thermal ^1H spectra where hydride signals were found to be extremely weak (see SI). This could explain the indifference in ^1H enhancement level observed when BnNH$_2$ was used as a co-ligand as also been previously shown by Lehmkuhl et al.[46] Moreover, NMR signals of BnNHD/BnNH$_2$ were found to be weakly enhanced by the SABRE process and consequently relaying the polarisation to the methanol via fast proton exchanges, which in turn may influenced the overall ^1H enhancement level of Odz achieved in this case.

Remarkably, a dramatic effect was observed when DMSO-d_6 was used (*sample-3*) as a co-ligand (25 mM) instead and the ^1H SABRE HP signal was recorded with an enhancement factors of 373-folds for the imidazole proton and 25-folds for the methyl protons as shown in Figure 2. The resulting ^1H spectra reveals that a new complex is successfully formed, which yields two hydride ligands with resonance frequencies at −22.36 ppm and −23.52 ppm originating from the neutral active species [IrCl (DMSO)(H)$_2$(IMes)(Odz)]. Here the DMSO ligand occupies the axial position (*trans* to IMes), whereas Odz and Cl occupy the equatorial positions (*trans* to hydrides ligands) of the iridium complex. The significant improvement of the proton enhancement level can be also attributed to the slower pH$_2$ and Odz exchange that is caused by the presence of DMSO as a co-ligand (see SI for more details).

2.2.3 | ^{15}N SABRE-SHEATH

Earlier studies on imidazole-based motifs such as metronidazole has proven to be extremely successful with ^{15}N SABRE-SHEATH producing up to 5 orders of signal enhancements.[16,19,27] Ornidazole contains similar imidazole motif within it and thereby indicating the suitability of this system. *Sample-1* (consisting of Odz and catalysts in CD$_3$OD) was shaken with fresh pH$_2$ inside a 0.5 μT magnetic field generated in the mu-metal chamber to initiate the SABRE-SHEATH effect. After 10 s of mixing, the sample tube was rapidly inserted inside the magnet for nitrogen-15 signal detection. Figure 3a
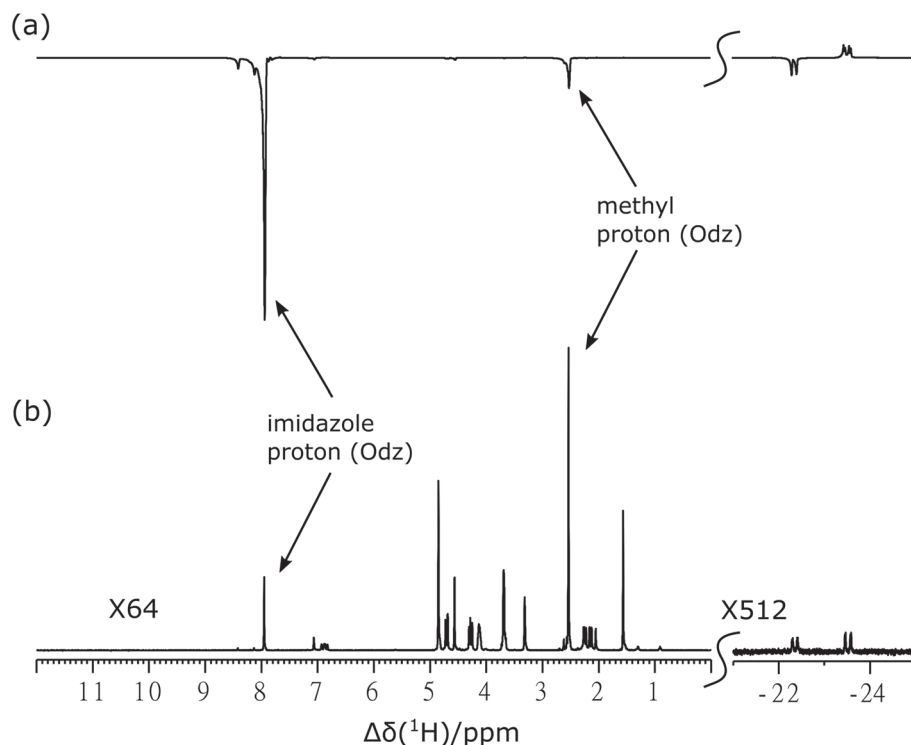
FIGURE 2 ^1H NMR spectra of Odz SABRE sample with 25 mM DMSO-d$_6$ added in the solution. (a) SABRE hyperpolarised spectrum after mixing with pH$_2$ ∼6 mT magnetic field and (b) corresponding signals at thermal equilibrium with respective vertical scales of 64 and 512 of the aromatic and hydride regions, respectively
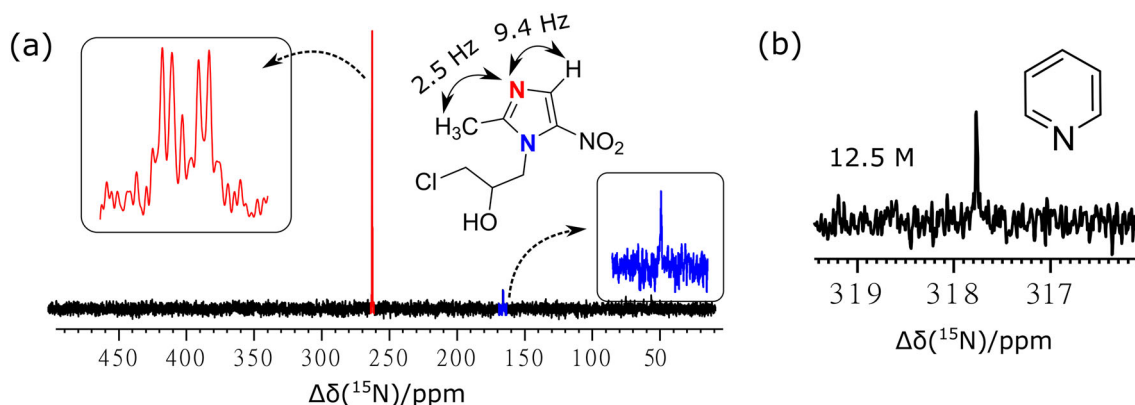
FIGURE 3 (a) $^{15}N\{^{1}H\}$ HP NMR spectra of Odz in CD_3OD (*sample-1*), showing two HP nitrogen-15 sites corresponding to the structure: red corresponds to the α-site, whereas blue refers to the β-site, with no signal originating from the NO_2 site of Odz. ^{15}N signal acquired without any ^{1}H decoupling (inset, red) reveals the fine splitting between the α-^{15}N and two nearby protons, as highlighted in the structure; (b) single scan thermal ^{15}N signal of neat (12.5 M) pyridine

demonstrates the efficiency of the procedure achieving hyperpolarised ^{15}N signal with an enhancement factor of 27,407 at 9.4 T (which corresponds to $P_{15N} \approx 9\%$, see SI for additional information). The enhancement factor of ^{15}N HP signal was calculated with reference to thermal ^{15}N signal of concentrated pyridine sample (12.5 M) with single scan and 300 s relaxation delay (Figure 3b). Whilst the α-nitrogen is benefitting from the strong *trans* hydride-^{15}N coupling constant of ~25 Hz, the SABRE-SHEATH effect can also be seen for the β-nitrogen that is 4-bonds away from the hydrides with a very small *J*-coupling constant to the hydrides. Also, working with natural abundance Odz means that the possibility of ^{15}N–^{15}N spin relays remain negligible in microtesla fields.[16,47] However, it should be noted that ^{15}N enrichment of Odz will likely render efficient ^{15}N polarisation of both the β and NO_2 sites of Odz.[19] The fine splitting of the HP α-nitrogen underlining the intramolecular *J*-couplings with the α-proton (2.5 Hz) and the methyl protons (9.4 Hz) can also be seen from the HP spectra. In order to find out the optimum field transfer condition, a magnetic field study was performed by changing the field inside the mu-metal chamber and recording the ^{15}N HP signal afterwards (see SI for experimental plot). For the α-nitrogen, the optimum transfer field was found to be 0.5 μT. We used this field for the rest of studies.

Sample-2 consisting of $BnNH_2$ as a co-ligand was then examined with this optimum SABRE-SHEATH condition. A much lower enhancement factor of 8862-folds ($P_{15N} \approx 3\%$,) was recorded as compared to *sample*-1 under same experimental procedures. The result indicates that the effect of fast H-D exchanges in conjunction with active relay mechanism propagated by $BnNH_2$ posing a negative impact on hyperpolarising the ^{15}N sites of Odz in this case.

Interestingly, although *sample-3* increased the polarisation level of ^{1}H significantly, when it was examined for SABRE-SHEATH, ^{15}N signal enhancements were found (~17,005-folds) to be lower as compared to *sample*-1, but nearly double that of *sample*-2.

A remarkable level of ^{15}N signal with 71,473-folds enhancement factor (translating to $P_{15N} \approx 23\%$) was achieved when dichloromethane-d_2 (CD_2Cl_2) was used as a polar aprotic solvent (*sample-4*). In CD_2Cl_2, H/D exchange is not possible, and thus the main active species is a neutral inorganic complex $[IrCl(H)_2(IMes)(Odz)_2]$, where one Odz and Cl ligand occupy the equatorial positions each, whereas a second Odz ligand binds to the axial position of the catalyst. The equatorial Odz then exchanges rapidly with the free Odz in the solution resulting in a broad ^{1}H and ^{15}N NMR signals (see SI for more details).

Figure 4a depicts the ^{15}N HP signals originating from the α-nitrogen of Odz under optimum SABRE-SHEATH field (0.5 μT) for sample 1–4. The corresponding enhancement factors and polarisation levels (Figure 4b) were calculated with reference to the thermal ^{15}N signal acquired from a neat pyridine sample of 12.5 M. Table 1 summarises the result and SI includes relevant spectral data.

2.2.4 | ^{15}N HP lifetimes

In general, ^{15}N offers a much longer T_1 lifetime compared to ^{1}H and therefore present an interesting prospect of longer lasting HP magnetisation that is essential for their further applications. Earlier Chekmenev and
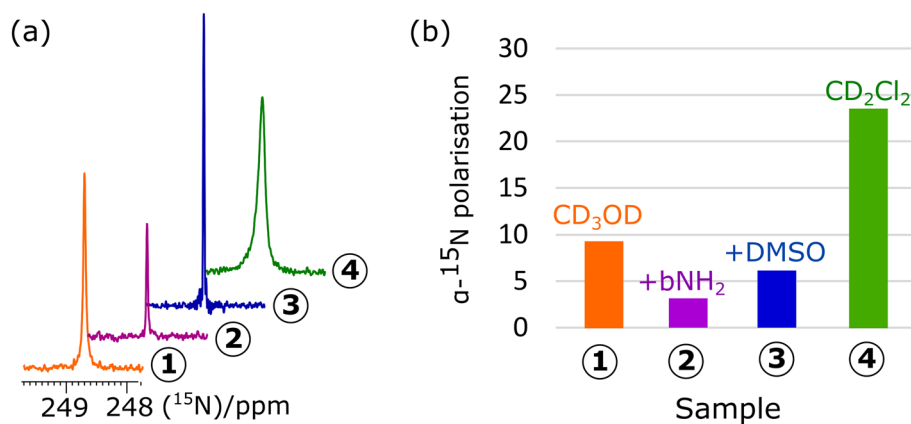
FIGURE 4 (a) HP $^{15}N\{^{1}H\}$ NMR signal (α-site) acquired at 0.5 mT SABRE-SHEATH field and (b) calculated net ^{15}N polarisation for *sample-1* to *sample-4*. HP enhancement levels were calculated with reference to the thermal ^{15}N signal acquired from a neat pyridine sample of 12.5 M (see SI for polarisation calculation)

TABLE I ^{1}H and ^{15}N enhancement levels achieved with different sample conditions and optimum SABRE (6 mT) and SABRE-SHEATH (0.5 μT) conditions, respectively

Sample	^{1}H (imidazole proton) enhancement factor	α-^{15}N enhancement factor	Net α-^{15}N polarisation
1	8	27,407	9%
2	23	8862	3%
3	373	17,005	6%
4	58	71,473	23%

Note: All measurements were made at 9.4 T and 298 K. Results are shown for the imidazole proton and α-nitrogen. The enhancement factor for the ^{1}H was calculated with reference to thermal signal of the same sample, whereas ^{15}N enhancements were calculated with reference to the thermal ^{15}N signal of a neat pyridine sample (see SI for enhancement factor calculation).

co-workers have reported ^{15}N lifetimes of HP metronidazole as ~10 min at 1.4 T under suitable experimental conditions.[19] Here we studied the lifetime of ^{15}N HP signal of *sample-4* under two different conditions. After polarising the sample at SABRE-SHEATH condition, the sample tube was rapidly inserted inside the magnet for signal detections by applying successive small flip angle (15°) pulses evenly spaced with 4 s inter-delays. An exponential fitting of the integrated signal yields a high-field (9.4 T) T_1 lifetime of the ^{15}N HP signal as 27.5 ± 2.7 s. This result is similar to what was achieved in the case of metronidazole and as reported the chemical shift anisotropy (CSA) dominates the relaxation mechanism at the high field.[16] The low-field T_1 measurement was carried out by a series of manually controlled experiments where after polarising the sample at optimum transfer field, it was kept at a field region of ~0.3 T for a variable time before inserting the sample at high-field magnet for immediate signal acquisition. A storage field of 0.3 T was chosen based on earlier work of Chekmenev and others, where it was shown that SABRE derived ^{15}N magnetisation poses much longer T_1 at these intermediary fields rather than at more conventional mT or μT fields.[18,22] A mono-exponential fitting of the integrated signal yields a T_1 of 110 ± 32 s, whereas a bi-exponential fitting gives a value of 186 ± 45 s. The large error

coefficients of these T_1 values can be attributed to the manual procedures of the experiments in addition to complicated relaxation spin dynamics as was also the case in high-field measurements. Figure 5 illustrates the normalised HP signal amplitude as a function of time at two different magnetic field storages. The fast decay of HP signal at low field during the first 10 s may be ascribed to the dynamic chemical exchange and aggressive diffusion mechanism that remain relevant during this period before stabilisation.
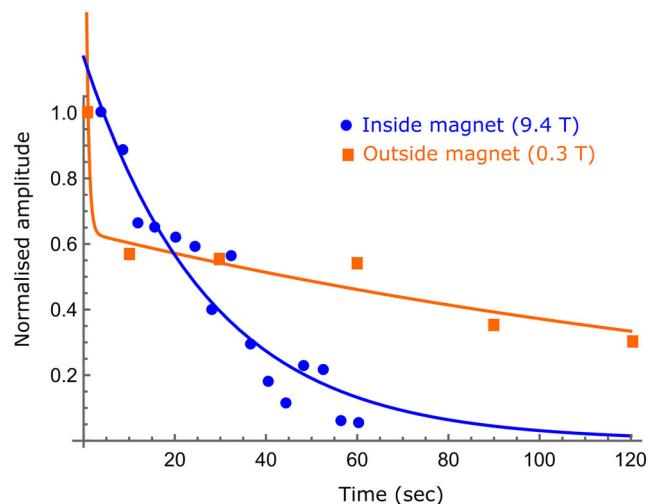
It should be possible to increase the T_1 lifetimes further by increasing the amount of the substrates as established earlier.[48] In addition, the quadrupolar effect of the α-nitrogen site plays a critical role as a relaxation sink to the spin lifetimes of the target spins.[25] Indeed, Chekmenev and co-workers have explored the effect of quadrupolar spins in relation to spin relays in SABRE and found that the lifetime of the target spins including of the distant nuclei can be significantly extended by labelling the nitrogen sites of the substrates.[19,47] When all the three nitrogen sites of metronidazole were labelled, an impressive 20 min spin lifetime was achieved for the NO_2 site of nitrogen.[19,49] We are currently in the process of understanding the complicated relaxation mechanism in such systems.

2.2.5 | ^{15}N HP signal in aqueous medium

The Ir-IMes catalyst is considered toxic and its complete removal from the HP solutions is imperative in order to make SABRE method fully biocompatible. An elegant method based on phase transfer catalysis was introduced by Reineri et al in relation to PHIP-Side Arm Hydrogenation technique, demonstrating the efficacy of such process into MRI applications after filtering the catalysts before an in vivo administration.[50,51] Thereafter, Iali

FIGURE 5 Normalised HP signal amplitude of ^{15}N NMR signals of *sample-4* observed after SABRE-SHEATH as a function of sample storage time. Data points were fitted to mono-exponential (blue solid curves) for high-field (9.4 T) storage and bi-exponential (orange solid curves) for low-field storages

et al described a similar technique in conjunction with SABRE, where simple N-heterocyclic substrates were shown to hyperpolarise into an emulsion of two immiscible solvents and following a natural phase separation procedure, hyperpolarised signals were detected from the water phase that contains very low traces of catalyst (in the order of $\mu M/dm^3$).[52] A slightly different approach of catalyst removal was followed by Kidd et al., where they applied chelating agents, for example, functionalised SiO_2 microparticles to extract the catalyst from HP solutions.[53] The phase separation process, however, can take significant time towards completion, it is therefore desirable to have HP nuclei with long T_1 to realise the full potential of this filtration procedure. HP ^{15}N nuclei may offer a convenient route to adopt this process, owing to its longer spin relaxation times. Here we demonstrate the phase separation technique in conjunction to SABRE-SHEATH of Odz revealing the hyperpolarised ^{15}N signal in water phase with minimal hint of catalyst contamination.

A sample was prepared by mixing 0.25 ml of CD_2Cl_2 solution containing 5 mM of catalyst and 25 mM of Odz with 0.35 ml of deuterium oxide (D_2O) solution containing 25 mM of Odz. A small amount of salt (2 mg, NaCl) was added to the solution to fasten up the separation process. The sample is then shaken with pH_2 inside the mu-metal chamber to instigate the SABRE-SHEATH process. The emulsified solution is then kept at a 0.3 T field where the phase separation begins almost immediately and leading to near perfect separation after ~30 s of wait. The sample was then rapidly inserted inside the magnet for NMR measurements. The phase separation process is readily
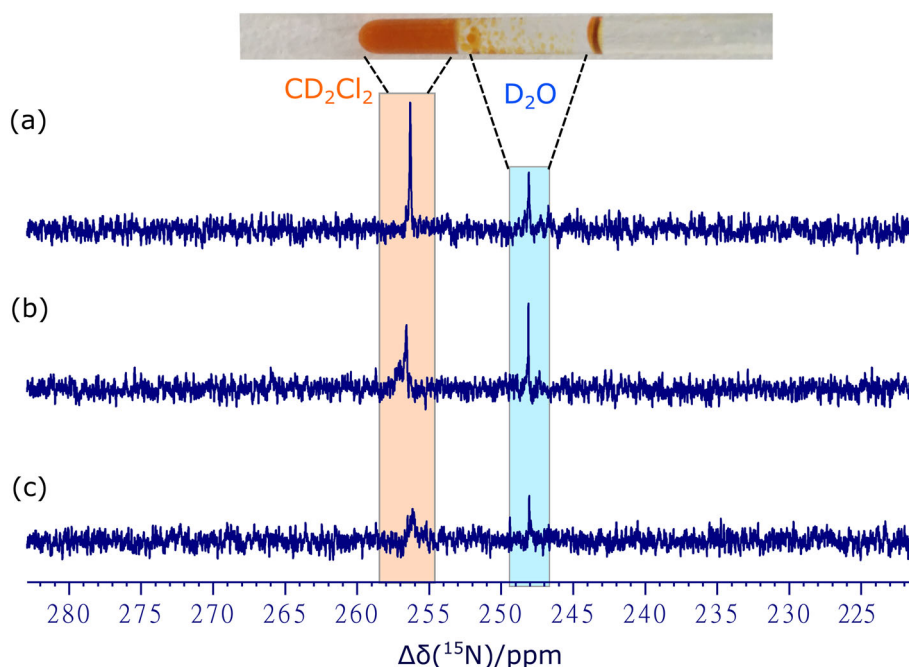
FIGURE 6 ^{15}N{^{1}H} NMR spectra (α-nitrogen) of Odz in bi-phasic solution after SABRE-SHEATH at 0.5 mT and waiting (at 0.3 T region) for (a) 30 s, (b) 45 s and (c) 60 s post pH_2 bubbling. Signal originating from the CD_2Cl_2 phase can be seen at the downfield (orange marked), whereas the signal from D_2O phase is seen towards the upfield (blue marked). A picture of the actual sample tube portraying the bi-phasic nature of the solution is shown above (inset)

noticeable by looking at the tube which forms an orange-coloured solution at the bottom half of the tube confirming the formation of SABRE active species, whereas the top half of the tube turns into a colourless solution over the separation period with little hints of organic bubbles. These imperfections could be potentially mitigated by use of sonication but was not done in this work. ^{15}N HP NMR spectra of the solution confirms the accomplishment of the separation process by revealing two chemically distinct species of resonances.[52] Figure 6 illustrates the success of the procedure showing ^{15}N hyperpolarised signal of Odz for an extended duration of time post solvent separation by retaining ca. 1% ^{15}N polarisation in the D2O phase after 1 min of wait time. A significant drop in ^{15}N HP signal was noticed. Nevertheless, the result confirms the feasibility of the phase separation approach in the context of SABRE-SHEATH and we are currently in the process of optimising the system by employing an automaticsample mixer in conjunction with faster phase extraction methods.

3 | CONCLUSION

In summary, we demonstrate a simple route to hyperpolarise natural abundant Odz, an important and routinely used antibiotics to generate strong ^{15}N signal with >4 orders of signal enhancements by employing a basic liquid-N$_2$ cooled pH_2 generator. When DMSO-d_6 was used as a co-ligand to the Odz, we observe >2 orders of enhancement in the ^1H HP signal compared to the standard SABRE protocol. A remarkable level of ^{15}N polarisation (23%) with ∼71,000-folds of enhancement factor was achieved when CD_2Cl_2 was used as a solvent. The ^{15}N lifetimes was found to be significantly longer at certain 'low' magnetic fields compared to both high-field and ultra-low field measurement, confirming the similar pattern that was achieved earlier for other ^{15}N nuclei. In the final refinement we employed a phase separation approach leading to detect ^{15}N hyperpolarised signal of Odz in the aqueous medium for an extended period of time. Further, the distinct separation in ^{15}N resonances originating from the organic solution and the aqueous phase can potentially be exploited in relation to sensing experiments including in HP in vivo studies.[54,55] This work highlights the attainment high levels of ^{15}N polarisation enabling the detection of nitrogen containing compounds even at natural abundance and with 50% enriched *para*-hydrogen. We envisage this approach to be expanded further with nitrogen containing biomolecules which when coupled with their longer lifetimes and catalyst removal technique, can be utilised towards biological applications.

ORCID

Soumya S. Roy https://orcid.org/0000-0002-9193-9712

REFERENCES

[1] J. H. Lee, Y. Okuno, S. Cavagnero, *J. Mag. Res.* **2014**, *241*, 18.

[2] P. Nikolaou, B. M. Goodson, E. Y. Chekmenev, *Chem. Eur. J.* **2015**, *21*, 3156.

[3] J. Kurhanewicz, D. B. Vigneron, J. H. Ardenkjaer-Larsen, J. A. Bankson, K. Brindle, C. H. Cunningham, F. A. Gallagher, K. R. Keshari, A. Kjaer, C. Laustsen, D. A. Mankoff, M. E. Merritt, S. J. Nelson, J. M. Pauly, P. Lee, S. Ronen, D. J. Tyler, S. S. Rajan, D. M. Spielman, L. Wald, X. L. Zhang, C. R. Malloy, R. Rizi, *Neoplasia* **2019**, *21*, 1.

[4] J. H. Ardenkjaer-Larsen, *J. Mag. Res.* **2016**, *264*, 3.

[5] C. R. Bowers, D. P. Weitekamp, *J. Am. Chem. Soc.* **1987**, *109*, 5541.

[6] T. C. Eisenschmid, R. U. Kirss, P. P. Deutsch, S. I. Hommeltoft, R. Eisenberg, J. Bargon, R. G. Lawler, A. L. Balch, *J. Am. Chem. Soc.* **1987**, *109*, 8089.

[7] J. B. Hovener, A. N. Pravdivtsev, B. Kidd, C. R. Bowers, S. Gloggler, K. V. Kovtunov, M. Plaumann, R. Katz-Brull, K. Buckenmaier, A. Jerschow, F. Reineri, T. Theis, R. V. Shchepin, S. Wagner, P. Bhattacharya, N. M. Zacharias, E. Y. Chekmenev, *Angew. Chem., Int. Ed.* **2018**, *57*, 11140.

[8] R. W. Adams, J. A. Aguilar, K. D. Atkinson, M. J. Cowley, P. I. P. Elliott, S. B. Duckett, G. G. R. Green, I. G. Khazal, J. Lopez-Serrano, D. C. Williamson, *Science* **2009**, *323*, 1708.

[9] K. L. Ivanov, A. N. Pravdivtsev, A. V. Yurkovskaya, H.-M. Vieth, R. Kaptein, *Prog. Nucl. Magn. Reson. Spectrosc.* **2014**, *81*, 1.

[10] A. N. Pravdivtsev, K. L. Ivanov, A. V. Yurkovskaya, P. A. Petrov, H.-H. Limbach, R. Kaptein, H.-M. Vieth, *J. Mag. Res.* **2015**, *261*, 73.

[11] W. Iali, P. J. Rayner, S. B. Duckett, *Sci. Adv.* **2018**, *4*. eaao6250

[12] P. J. Rayner, S. B. Duckett, *Angew. Chem., Int. Ed.* **2018**, *57*, 6742.

[13] S. S. Roy, K. M. Appleby, E. J. Fear, S. B. Duckett, *J. Phys. Chem. Lett.* **2018**, *9*, 1112.

[14] W. Iali, S. S. Roy, B. J. Tickner, F. Ahwal, A. J. Kennerley, S. B. Duckett, *Angew. Chem., Int. Ed.* **2019**, *58*, 10271.

[15] T. Theis, M. L. Truong, A. M. Coffey, R. V. Shchepin, K. W. Waddell, F. Shi, B. M. Goodson, W. S. Warren, E. Y. Chekmenev, *J. Am. Chem. Soc.* **2015**, *137*, 1404.

[16] D. A. Barskiy, R. V. Shchepin, A. M. Coffey, T. Theis, W. S. Warren, B. M. Goodson, E. Y. Chekmenev, *J. Am. Chem. Soc.* **2016**, *138*, 8080.

[17] J. F. Colell, A. W. Logan, Z. Zhou, R. V. Shchepin, D. A. Barskiy, G. X. Ortiz Jr., Q. Wang, S. J. Malcolmson, E. Y. Chekmenev, W. S. Warren, T. Theis, *J. Phys. Chem. C* **2017**, *121*, 6626.

[18] R. V. Shchepin, L. Jaigirdar, E. Y. Chekmenev, *J. Phys. Chem. C* **2018**, *122*, 4984.

[19] R. V. Shchepin, J. R. Birchall, N. V. Chukanov, K. V. Kovtunov, I. V. Koptyug, T. Theis, W. S. Warren, J. G. Gelovani, B. M. Goodson, S. Shokouhi, M. S. Rosen, Y. F. Yen, W. Pham, E. Y. Chekmenev, *Chem. Eur. J.* **2019**, *25*, 8829.

[20] M. E. Gemeinhardt, M. N. Limbach, T. R. Gebhardt, C. W. Eriksson, S. L. Eriksson, J. R. Lindale, E. A. Goodson, W. S. Warren, E. Y. Chekmenev, B. M. Goodson, *Angew. Chem., Int. Ed.* **2020**, *59*, 418.

[21] O. G. Salnikov, N. V. Chukanov, A. Svyatova, I. A. Trofimov, M. S. H. Kabir, J. G. Gelovani, K. V. Kovtunov, I. V. Koptyug, E. Y. Chekmenev, *Angew. Chem., Int. Ed.* **2021**, *60*, 2406.

[22] S. S. Roy, P. J. Rayner, M. J. Burns, S. B. Duckett, *J. Chem. Phys.* **2020**, *152*, 014201.

[23] A. M. Olaru, A. Burt, P. J. Rayner, S. J. Hart, A. C. Whitwood, G. G. R. Green, S. B. Duckett, *Chem. Commun.* **2016**, *52*, 14482.

[24] V. V. Zhivonitko, I. V. Skovpin, I. V. Koptyug, *Chem. Commun.* **2015**, *51*, 2506.

[25] D. A. Barskiy, R. V. Shchepin, C. P. N. Tanner, J. F. P. Colell, B. M. Goodson, T. Theis, W. S. Warren, E. Y. Chekmenev, *ChemPhysChem* **2017**, *18*, 1493.

[26] R. V. Shchepin, B. M. Goodson, T. Theis, W. S. Warren, E. Y. Chekmenev, *ChemPhysChem* **2017**, *18*, 1961.

[27] M. Fekete, F. Ahwal, S. B. Duckett, *J. Phys. Chem. B* **2020**, *124*, 4573.

[28] T. Theis, G. X. Ortiz, A. W. Logan, K. E. Claytor, Y. Feng, W. P. Huhn, V. Blum, S. J. Malcolmson, E. Y. Chekmenev, Q. Wang, W. Warren, *Sci. Adv.* **2016**, *2*. e1501438

[29] C. Cudalbu, A. Comment, F. Kurdzesau, R. B. van Heeswijk, K. Uffmann, S. Jannin, V. Denisov, D. Kirik, R. Gruetter, *Phys. Chem. Chem. Phys.* **2010**, *12*, 5818.

[30] W. Jiang, L. Lumata, W. Chen, S. Zhang, Z. Kovacs, A. D. Sherry, C. Khemtong, *Sci. Rep.* **2015**, *5*, 9104.

[31] H. Nonaka, R. Hata, T. Doura, T. Nishihara, K. Kumagai, M. Akakabe, M. Tsuda, K. Ichikawa, S. Sando, *Nat. Commun.* **2013**, *4*, 2411.

[32] M. Sköld, H. Gnarpe, L. Hillström, *Br. J. Vener. Dis.* **1977**, *53*, 44.

[33] D. E. Schwartz, F. Jeunet, *Chemotherapy* **1976**, *22*, 19.

[34] M. H. Wilcox, in *Infectious diseases*, eds. J. Cohen, W. G. Powderly and S. M. Opal, Elsevier, **2017**, pp. 1261–1263. https://doi.org/10.1016/B978-0-7020-6285-8.00147-7

[35] M. J. Cowley, R. W. Adams, K. D. Atkinson, M. C. R. Cockett, S. B. Duckett, G. G. R. Green, J. A. B. Lohman, R. Kerssebaum, D. Kilgour, R. E. Mewis, *J. Am. Chem. Soc.* **2011**, *133*, 6134.

[36] R. V. Shchepin, D. A. Barskiy, A. M. Coffey, T. Theis, F. Shi, W. S. Warren, B. M. Goodson, E. Y. Chekmenev, *Acs Sensors* **2016**, *1*, 640.

[37] M. Fekete, P. J. Rayner, G. G. R. Green, S. B. Duckett, *Magn. Reson. Chem.* **2017**, *55*, 944.

[38] R. V. Shchepin, D. A. Barskiy, A. M. Coffey, M. A. Feldman, L. M. Kovtunova, V. I. Bukhtiyarov, K. V. Kovtunov, B. M. Goodson, I. V. Koptyug, E. Y. Chekmenev, *ChemistrySelect* **2017**, *2*, 4478.

[39] R. V. Shchepin, M. L. Truong, T. Theis, A. M. Coffey, F. Shi, K. W. Waddell, W. S. Warren, B. M. Goodson, E. Y. Chekmenev, *J. Phys. Chem. Lett.* **2015**, *6*, 1961.

[40] A. S. Kiryutin, A. V. Yurkovskaya, H. Zimmermann, H. M. Vieth, K. L. Ivanov, *Magn. Reson. Chem.* **2018**, *56*, 651.

[41] S. Knecht, K. L. Ivanov, *J. Chem. Phys.* **2019**, *150*, 124106.

[42] P. M. Richardson, W. Iali, S. S. Roy, P. J. Rayner, M. E. Halse, S. B. Duckett, *Chem. Sci.* **2019**, *10*, 10607.

[43] R. V. Shchepin, D. A. Barskiy, D. M. Mikhaylov, E. Y. Chekmenev, *Bioconjugate Chem.* **2016**, *27*, 878.

[44] W. Iali, P. J. Rayner, A. Alshehri, A. J. Holmes, A. J. Ruddlesden, S. B. Duckett, *Chem. Sci.* **2018**, *9*, 3677.

[45] B. J. Tickner, R. O. John, S. S. Roy, S. J. Hart, A. C. Whitwood, S. B. Duckett, *Chem. Sci.* **2019**, *10*, 5235.

[46] S. Lehmkuhl, M. Emondts, L. Schubert, P. Spannring, J. Klankermayer, B. Blumich, P. P. M. Schleker, *ChemPhysChem* **2017**, *18*, 2426.

[47] R. V. Shchepin, L. Jaigirdar, T. Theis, W. S. Warren, B. M. Goodson, E. Y. Chekmenev, *J. Phys. Chem. C* **2017**, *121*, 28425.

[48] S. S. Roy, P. J. Rayner, P. Norcott, G. G. R. Green, S. B. Duckett, *Phys. Chem. Chem. Phys.* **2016**, *18*, 24905.

[49] J. R. Birchall, M. S. H. Kabir, O. G. Salnikov, N. V. Chukanov, A. Svyatova, K. V. Kovtunov, I. V. Koptyug, J. G. Gelovani, B. M. Goodson, W. Pham, E. Y. Chekmenev, *Chem. Commun.* **2020**, *56*, 9098.

[50] F. Reineri, T. Boi, S. Aime, *Nat. Commun.* **2015**, *6*, 5858.

[51] E. Cavallari, C. Carrera, M. Sorge, G. Bonne, A. Muchir, S. Aime, F. Reineri, *Sci. Rep.* **2018**, *8*, 8366.

[52] W. Iali, A. M. Olaru, G. G. R. Green, S. B. Duckett, *Chem. Eur. J.* **2017**, *23*, 10491.

[53] B. E. Kidd, J. L. Gesiorski, M. E. Gemeinhardt, R. V. Shchepin, K. V. Kovtunov, I. V. Koptyug, E. Y. Chekmenev, B. M. Goodson, *J. Phys. Chem. C* **2018**, *122*, 16848.

[54] P. Bhattacharya, E. Y. Chekmenev, W. F. Reynolds, S. Wagner, N. Zacharias, H. R. Chan, R. Bunger, B. D. Ross, *NMR Biomed.* **2011**, *24*, 1023.

[55] R. T. Branca, T. He, L. Zhang, C. S. Floyd, M. Freeman, C. White, A. Burant, *Proc. Nat. Acad. Sci.* **2014**, *111*, 18001.

SUPPORTING INFORMATION

Additional supporting information may be found online in the Supporting Information section at the end of this article.